International Journal of Electrical and Computer Engineering (IJECE)
Vol. 13, No. 5, October 2023, pp. 5066~5075
ISSN: 2088-8708, DOI: 10.11591/ijece.v13i5.pp5066-5075

Sensor fault reconstruction for wind turbine benchmark model using a modified sliding mode observer

Mohammed Taouil[1], Abdelghani El Ougli[2], Belkassem Tidhaf[1], Hafida Zrouri[1]
[1]Embedded Systems, Renewable Energy and Artificial Intelligence Team, National School of Applied Sciences, Mohammed First University, Oujda, Morocco
[2]Computer Science, Signal, Automation and Cognitivism Laboratory, Faculty of Science Sidi Mohamed Ben Abdellah University, Fez, Morocco

Article Info

Article history:

Received Sep 27, 2022
Revised Feb 22, 2023
Accepted Mar 9, 2023

Keywords:

Sensor fault reconstruction
Separate faults
Simultaneous faults
Sliding mode observer
Wind turbine model

ABSTRACT

This paper proposes a fault diagnosis scheme applied to a wind turbine system. The technique used is based on a modified sliding mode observer (SMO), which permits the reconstruction of actuator and sensor faults. A wind turbine benchmark with a real sequence of wind speed is exploited to validate the proposed fault detection and diagnosis scheme. Rotor speed, generator speed, blade pitch angle, and generator torque have different orders of magnitude. As a result, the dedicated sensors are susceptible to faults of quite varying magnitudes, and estimating simultaneous sensor faults with accuracy using a classical SMO is difficult. To address this issue, some modifications are made to the classic SMO. In order to test the efficiency of the modified SMO, several sensor fault scenarios have been simulated, first in the case of separate faults and then in the case of simultaneous faults. The simulation results show that the sensor faults are isolated, detected, and reconstructed accurately in the case of separate faults. In the case of simultaneous faults, with the proposed modification of SMO, the faults are precisely isolated, detected, and reconstructed, even though they have quite different amplitudes; thus, the relative gap does not exceed 0.08% for the generator speed sensor fault.

Corresponding Author:

Mohammed Taouil
Embedded Systems, Renewable Energy and Artificial Intelligence Team, National School of Applied Sciences, Mohammed First University
BP 473 Al Qods University Complex Oujda, Morocco
Email: t123med@hotmail.fr

1. INTRODUCTION

In the last decade, the most rapidly expanding renewable energy sources are wind turbines, supplied by an entirely arbitrary wind speed, operating in uncertain environments, nonlinear dynamics, and exposure to considerable disturbances are key properties of these systems [1], [2]. Several recent studies have been conducted to improve the power coefficient of wind turbines as well as electricity production, blade profile and augmentation strategies using optimization approaches based on artificial intelligence (AI) have been addressed [3], [4]. Notwithstanding the implementation of advanced technology in modern wind turbines, the maintenance of these turbines is still long and costly, which influences their electricity production [5].

Odgaard *et al.* presented two wind turbine benchmark models (WTBMs) in 2009 [6] and 2013 [7], the second model is more realistic. Several research papers have been published in fault detection and isolation (FDI), and fault tolerant control (FTC) based on these WTBMs [8]–[11]. The main objective of an FDI system is to raise an alarm when an abnormal operation occurs in the monitored process and to locate its source. A widely studied methodology is the observer-based approach, which analyzes the residuals that represent the difference between the actual and observer outputs of the monitored system [12], [13]. In this paper, an observer class known as the sliding mode observer [14] is adopted. This observer class aims to reconstruct the fault instead of examining the residual.

An unknown input proportional integral observer for decoupling the unknown input was established in Sun [15], and an optimization of it is introduced to lessen the effects of sensor noise, the actuator faults of the WTBM were also estimated using the suggested observer. A Kalman-like observer and support vector machines-based FDI system were proposed in [16], [17]. Shi and Patton [18] proposed an observer based active fault tolerant control (AFTC) approach. By modeling the wind turbine as a linear parameter varying (LPV) model using linear matrix inequality linear matrix inequality (LMI), to evaluate the system states and faults, an extended state observer was established. To examine some faults in wind turbines, a deep learning fault detection and classification method based on the time series analysis method and convolutional neural networks (CNN) is provided [19]. Changes in wind turbine blade vibration responses WTB can be used to detect the presence of damage. Xu *et al.* [20] introduced a probabilistic analysis approach for wind turbine damage detection.

Sliding mode observers sliding mode observers (SMOs) are characterized by robustness to disturbances and modeling uncertainties as well as their ability to estimate unknown inputs. SMOs have been widely used for FDI [14], [21]–[24]. Using a Takagi-Sugeno SMO, the actuator parameter faults in the WTBM were only partially identified and reconstructed [25], the reconstruction's accuracy needs to be improved because the method lacks robustness regarding model uncertainty. SMO is used by Rahnavard *et al.* [26], [27] to address the fault detection (FD) of sensors and actuators in the WTBM.

In contrast to WTBM-based approaches that merely detect and isolate the fault without providing any information on its magnitude, this paper proposes an FDI scheme that, in addition to faithfully reconstructing the fault, provides the exact magnitude, making it exploitable in FTC schemes that require knowledge of the fault magnitude. A modified fault estimation scheme based on the SMO is presented in this paper, particularly to detect, isolate, and estimate the sensor faults of the WTBM. The proposed modification is related to the discontinuous switching term of the observer, which allows an accurate reconstruction, especially in the case of simultaneous faults. The aerodynamic torque is considered as an input, and the MATLAB/Simulink environment is used to implement the simulations. The paper is structured as: section 2 briefly describes the WTBM, section 3 presents the fault estimation scheme along with modifications to the SMO and numerical values of its parameters, section 4 addresses fault scenarios and simulation results, and section 5 concludes the paper.

2. WIND TURBINE MODEL

The model considered is similar to the one studied in [7], it is a horizontal axis wind turbine with three blades, Figure 1 depicts a system overview of this system. This benchmark model contains the following subsystems: blade and pitch system, drive train, converter, and generator, the wind turbine's aerodynamic characteristics are strongly dependent on the blade pitch angles, the rotor speed, and the wind speed, which is the driving force of the wind power system. The resulting aerodynamic torque is transmitted from the rotor to the generator via the drive train, and at the output, the electrical energy is obtained from the converter. Depending on the different operating requirements, a controller is set up to control the blade pitch angles and the generator torque [28].

2.1. Blade and pitch subsystem

This block contains the aerodynamic model, blades, and pitch system. The aerodynamic torque is given by the relation:

$$\tau_r = \frac{\rho\pi R^3 C_q(\lambda,\beta) v_w^2}{2} \tag{1}$$

$$C_q(\lambda,\beta) = \frac{C_p(\lambda,\beta)}{\lambda} \tag{2}$$

$C_q\,(\lambda,\beta)$ is the torque coefficient, the profile used for $C_q\,(\lambda,\beta)$ is shown in Figure 2, C_q is a nonlinear function as a function of the pitch angle β and on tip speed ratio λ, therefore τ_r is a nonlinear function of β, λ and the wind speed v_w.

The pitch system is a hydraulic system consisting of three identical actuators, each with an internal controller, the actuator i adjusts the pitch angle β_i(i=1, 2, 3) of the blades by rotating them. This subsystem can be represented by the following second order transfer function:

$$\frac{\beta_i(s)}{\beta_{r,i}} = \frac{\omega_{ni}^2}{s^2+2.\xi_i.\omega_{ni}.s+\omega_{ni}^2} \tag{3}$$

where β_i denote the pitch angle, $\beta_{r,i}$ denote the reference to the pitch angle, ω_{ni} denote the natural frequency of the pitch actuator model [rad/s], and ξ_i denote the damping ratio of the pitch actuator model. All β_i, all ω_{ni} and all ξ_i are equal in free fault, otherwise are different. In the following only one pitch actuator is considered.

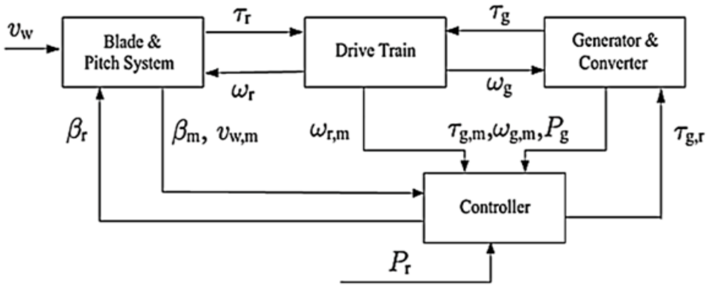

Figure 1. Overview of the wind turbine system [7]

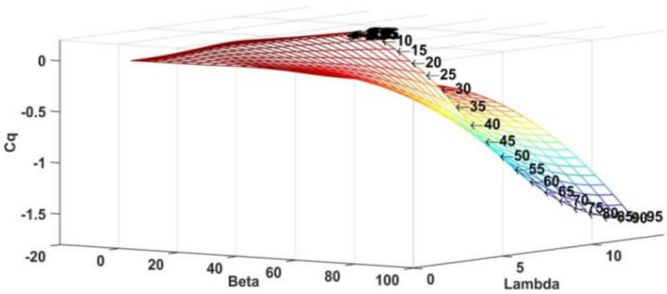

Figure 2. C_q mapping

2.2. Drive train subsystem

The drive train allows to transfer the aerodynamic torque to the generator to ensure a high speed of rotation required by the generator, the model is built of a slow shaft and a fast shaft linked by a multiplier (the gearbox). This subsystem is modeled by (4)-(6):

$$\begin{cases} J_g.\dot{\omega}_g = -\left(\frac{\eta_{dt}B_{dt}}{N_g^2} + B_g\right)\omega_g + \frac{\eta_{dt}B_{dt}}{N_g}\omega_r + \frac{\eta_{dt}K_{dt}}{N_g}\theta - \tau_g, & (4) \\ J_r\dot{\omega}_r = \frac{B_{dt}}{N_g}\omega_g - (B_{dt} + B_r)\omega_r - K_{dt}\theta + \tau_r\ , & (5) \\ \dot{\theta} = \omega_r - \frac{1}{N_g}\omega_g. & (6) \end{cases}$$

Table 1 gathers the meaning of the parameters evoked in the (4)-(6).

Table 1. Drive train parameter description [7]

ω_g Generator angular speed	τ_g Generator torque	J_g Generator moment of inertia	B_g Generator viscous friction
N_g Gear ratio	θ torsion angle of the drive train	ω_r Rotor angular speed	τ_r Rotor torque
J_r moment of inertia of the low-speed shaft	B_r viscous friction of the low-speed shaft	K_{dt} torsion stiffness of the drive train	B_{dt} torsion damping coefficient of the drive train

2.3. Generator and converter subsystem

In this subsystem we have a mechanical to electrical conversion, the converter and the generator are modeled by a transfer function of 1st order:

$$\frac{\tau_g}{\tau_{gref}} = \frac{1}{1+{}^{1}/_{\alpha_{gc}} s} \tag{7}$$

where τ_g is the generator torque, τ_{gref} is the reference generator torque, and ${}^{1}/_{\alpha_{gc}}$ is the first order system's time constant. The power available at the generator output is given by (8):

$$P_g = \eta_g . \omega_g . \tau_g \tag{8}$$

η_g denotes the generator's efficiency.

By integrating the subsystems described above, the wind system is modeled in the state space as (9), (10):

$$\begin{cases} \dot{x}(t) = A\,x(t) + B\,u(t), & (9) \\ y(t) = C\,x(t). & (10) \end{cases}$$

where $x = [\omega_g \quad \omega_r \quad \theta\, \dot{\beta} \quad \beta \quad \tau_g]^T$ is the state vector, $u = [\tau_{gref} \quad \tau_r \quad \beta_r]^T$ denote the control input vector,

$$B = \begin{bmatrix} 0 & 0 & 0 \\ 0 & \frac{1}{J_g} & 0 \\ 0 & 0 & 0 \\ 0 & 0 & \omega_n^2 \\ 0 & 0 & 0 \\ \alpha_{gc} & 0 & 0 \end{bmatrix}, C = \begin{bmatrix} 1 & 0 & 0 & 0 & 0 & 0 \\ 0 & 1 & 0 & 0 & 0 & 0 \\ 0 & 0 & 0 & 1 & 0 & 0 \\ 0 & 0 & 0 & 0 & 1 & 0 \\ 0 & 0 & 0 & 0 & 0 & 1 \end{bmatrix},$$

$$A = \begin{bmatrix} a_{11} & \frac{\eta_{dt} B_{dt}}{N_g J_g} & \frac{\eta_{dt} K_{dt}}{N_g J_g} & 0 & 0 & -\frac{1}{J_g} \\ \frac{B_{dt}}{N_g J_r} & -\frac{B_{dt} + B_r}{J_r} & -\frac{K_{dt}}{J_r} & 0 & 0 & 0 \\ -\frac{1}{N_g} & 1 & 0 & 0 & 0 & 0 \\ 0 & 0 & 0 & -2\xi\omega_n & -\omega_n^2 & 0 \\ 0 & 0 & 0 & 1 & 0 & 0 \\ 0 & 0 & 0 & 0 & 0 & -\alpha_{gc} \end{bmatrix},$$

$$a_{11} = -\frac{\frac{\eta_{dt} B_{dt}}{N_g^2} + B_g}{J_g}.$$

3. FAULT ESTIMATION SCHEME

3.1. Sliding mode observer design

Consider the system of (11) and (12) which describes a nominal linear system vulnerable to sensor and actuator faults:

$$\begin{cases} \dot{x}(t) = A\,x(t) + B\,u(t) + D\,f_{act}(t)\,, & (11) \\ y(t) = C\,x(t) + f_{sen}(t). & (12) \end{cases}$$

where, $A \in \mathbb{R}^{n\times n}$, $B \in \mathbb{R}^{n\times m}$, $C \in \mathbb{R}^{p\times n}$, $D \in \mathbb{R}^{n\times q}$, with $p \geq q$ and the matrices B, C and D are full rank. The functions f_{act} and f_{sen} present respectively an actuator fault and a sensor fault, f_{act} and f_{sen} are bounded. A priori, only the u(t) and y(t) signals are provided, and it is assumed that the system's state is unknown. The objective is to synthesize an observer that allows for an estimated state vector $\hat{x}$ and an estimated output vector $\hat{y}$, such that the output error: $\varepsilon_y(t) = \hat{y}(t) - y(t)$ tends to zero in a finite time when the sliding mode is attained, even in the presence of faults.

It is shown in [14] that a change in coordinates exists $x \rightarrow \hat{T}.x$ such that in the new coordinate system, the previous system is written as (13)-(15):

$$\begin{cases} \dot{x}_1 = \mathcal{A}_{11}x_1 + \mathcal{A}_{12}x_2 + B_1 u, & (13) \\ \dot{x}_2 = \mathcal{A}_{21}x_1 + \mathcal{A}_{22}x_2 + B_2 u + D_2 f_{act}, & (14) \\ y = x_2 . & (15) \end{cases}$$

where $\mathcal{A}_{11}$ is stable

The coordinate system above will be used as a platform for the design of a SMO. The system of (11) and (12) in f_{act} undergoes two transformations, the first one with the matrix T and the second one with T_* so $\hat{T} = T_*.T$, T and T_* can be calculated by (16) and (17), more details can be found in [14], [21].

$$T = \begin{bmatrix} I_{n-p} & T_{12} \\ 0 & T_0 \end{bmatrix} \tag{16}$$

$$T_* = \begin{bmatrix} I_{n-p} & L_* \\ 0 & T_0^T \end{bmatrix} \tag{17}$$

Finally, the resulting structure is:

$$\dot{\hat{x}} = A\hat{x} + Bu - G_l\varepsilon_y + G_n\nu \tag{18}$$

where the gains G_l and G_n are calculated as (19):

$$G_l = \hat{T}^{-1}\begin{bmatrix} \mathcal{A}_{12} \\ \mathcal{A}_{22} - \mathcal{A}_{22}^s \end{bmatrix},\ G_n = \hat{T}^{-1}\begin{bmatrix} 0 \\ I_p \end{bmatrix} \tag{19}$$

$\mathcal{A}_{22}^s$ is a stable design matrix, let $P_2 \in \mathbb{R}^{p\times p}$ be symmetric positive definite Lyapunov matrix for $\mathcal{A}_{22}^s$ then the discontinuous injection switching vector ν is defined by (20):

$$\nu = \begin{cases} -\kappa \|D_2\| \frac{P_2\varepsilon_y}{\|P_2\varepsilon_y\|}, & if\ \varepsilon_y \neq 0 \\ 0 & otherwise \end{cases} \tag{20}$$

where κ is a positive scalar greater than the norm of the function that represents the fault. Ultimately, the sensorand actuator faults that have been reconstructed can be roughly estimated [16], [29] by (21), (22):

$$\hat{f}_{act} \approx -\kappa\|D_2\|({D_2}^T D_2)^{-1}D_2^T \frac{P_2\varepsilon_y}{\|P_2\varepsilon_y\|+\delta} \tag{21}$$

$$\hat{f}_{sen} \approx (\mathcal{A}_{22} - \mathcal{A}_{21}{\mathcal{A}_{11}}^{-1}\mathcal{A}_{12})^{-1}\kappa\|D_2\| \frac{P_2\varepsilon_y}{\|P_2\varepsilon_y\|+\delta} \tag{22}$$

The matrix D is chosen such that: D=B.

3.2. Modifications for the observer

The outputs of the wind turbine have very different orders of magnitude $10^2 rad/s, 1 rad/s$, $1deg$, and $10^4 N.m$ respectively for $\omega_g, \omega_r, \beta$ *and* τ_g, the reconstructed sensor and actuator faults are given by (21) and (22). These two relations shows that the reconstructed faults are highly dependent on the scalar gain, whose value is roughly equal to the fault magnitude's maximum value. The choice of κ changes according to the considered output and its value must be chosen with precision by the designer. Therefore, in the classical SMO structure, the parameter is taken as fixed, which introduces a limitation for the fault reconstruction.

In f_{act}, choosing a fixed κ does not allow for precise reconstruction of the faults of all the outputs; thus, it is necessary to redefine κ to adapt to each output, which is impractical and a priori inaccessible in the case where multiple faults affect multiple outputs at the same time. To remedy this problem, a modification to the parameter κ is proposed to be replaced by: $\frac{\alpha}{\|D_2\|}\left\|P_2\varepsilon_y\right\|$ and the switching term become:

$$\nu = -\alpha \left\| P_2 \varepsilon_y \right\| \frac{P_2 \varepsilon_y}{\left\| P_2 \varepsilon_y \right\| + \delta} \tag{24}$$

where α is a scalar is taken equal to $\frac{1}{450}$ and δ is a small scalar.

3.3. Observer design

The main source of the wind system's energy is the aerodynamic torque, which is obtained from relation (1) and represents the 2nd input for (9), the 1st and 3rd inputs are provided by the wind turbine controller. The technical specifications and parameter numerical values of the wind turbine simulated in this paper are given in Odgaard *et al.* [7]. The proposed observer has the structure (18), considering the modification of the switching term (24) and putting the system of (11) and (12) in the canonical forms (13), (14), and (15). Using an algorithm similar to the one described in [21], the obtained state space matrices:

$$\mathcal{A} = \begin{bmatrix} -4 & 1.07e^{-2} & -9.99e^{-1} & 0 & 0 & -1.45e^{-7} \\ -7.06e^{4} & 3.88 & 2.03e^{-2} & 0 & 0 & -2.56e^{-3} \\ 49.09 & -2.77e^{-3} & -1.42e^{-5} & 0 & 0 & 0 \\ 0 & 0 & 0 & -13.3 & -1.23e^{2} & 0 \\ 0 & 0 & 0 & 1 & 0 & 0 \\ 0 & 0 & 0 & 0 & 0 & -50 \end{bmatrix},$$

$$\mathcal{D} = \mathcal{B} = \begin{bmatrix} 0 & 0 & 0 \\ 0 & 0 & 0 \\ 0 & 1.81e^{-8} & 0 \\ 0 & 0 & 1.234e^{2} \\ 0 & 0 & 0 \\ 50 & 0 & 0 \end{bmatrix}, \mathcal{C} = \begin{bmatrix} 0 & 1 & 0 & 0 & 0 & 0 \\ 0 & 0 & 1 & 0 & 0 & 0 \\ 0 & 0 & 0 & 1 & 0 & 0 \\ 0 & 0 & 0 & 0 & 1 & 0 \\ 0 & 0 & 0 & 0 & 0 & 1 \end{bmatrix}.$$

The design parameters of the observer are taken as:

$$\mathcal{A}_{22}^{s} = \begin{bmatrix} -1e^{-2} & 0 & 0 & 0 & 0 \\ 0 & -2e^{-2} & 0 & 0 & 0 \\ 0 & 0 & -1e^{-2} & 0 & 0 \\ 0 & 0 & 0 & -1e^{-2} & 0 \\ 0 & 0 & 0 & 0 & -1e^{-2} \end{bmatrix}, \text{ and } \delta = 1e^{-6}$$

The gains obtained:

$$G_l = \begin{bmatrix} 3.893 & 2.03e^{-2} & 0 & 0 & -2.6e^{-3} \\ -2.8e^{-3} & 2e^{-2} & 0 & 0 & 0 \\ -1.5e^{-2} & 1 & 0 & 0 & 0 \\ 0 & 0 & -13.32 & -1.23e^{2} & 0 \\ 0 & 0 & 1 & 1e^{-2} & 0 \\ 0 & 0 & 0 & 0 & -49.99 \end{bmatrix}, G_n \begin{bmatrix} 1.234e^{2} & 0 & 0 & 0 & 0 \\ 0 & 1.234e^{2} & 0 & 0 & 0 \\ 7e^{-3} & 0 & 0 & 0 & 0 \\ 0 & 0 & 1.234e^{2} & 0 & 0 \\ 0 & 0 & 0 & 1.234e^{2} & 0 \\ 0 & 0 & 0 & 0 & 1.234e^{2} \end{bmatrix}$$

4. SIMULATION RESULTS

4.1. Wind input

The wind speed profile adopted in the simulation shown in Figure 3 is highly random and issued from a wind park's real wind speed measurement [7]. The wind speed considered covers a range of 3-18 m/s, which represents a good coverage of the normal operation of a wind turbine. Depending on the wind speed, in the interval (3, 12.5 m/s) the power generated by the wind turbine will be optimized, the wind turbine will be controlled to maintain a constant energy production in (12.5, 25 m/s), and if the speed exceeds 25 m/s the wind turbine will be parked in order to avoid any damage.

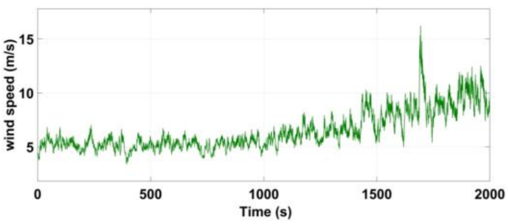

Figure 3. The random wind speed profile considered in the simulation

4.2. Sensor fault reconstruction

The objective is to reconstruct sensor faults, $f_{act}(t)$ is considered null in (11), four sensors are implemented to measure generator speed (ω_g), rotor speed (ω_r), blade pitch angle (β), and generator torque (τ_g), for each sensor, a fault is proposed, in the last case, the faults are considered simultaneously, the magnitude of the fault is chosen in a logical way according to the amplitude of the variable considered, and it is noted that the fault profile is a priori unknown by the system. The sensor faults simulated in this paper are the following:

Case 1: Figure 4 (fault case 1) shows the real and estimated faults of the generator torque sensor, which starts at 100 s and ends at 255 s; this fault realizes a constant amplitude bias, the maximum real fault amplitude is 400 N.m, this value represents 10% of the maximum value of the generator torque in the considered interval, the obtained result shows that the reconstructed fault follows faithfully and accurately the real fault.

Case 2: The generator speed sensor fault is reconstructed. It runs from 400 to 600 s as shown in Figure 4 (fault case 2). It is an intermittent fault that realizes a constant amplitude bias with maximum amplitude of 25 rad/s, which represents 32% of the maximum value of the generator speed in the considered interval. The results of the simulation show that the fault is reconstructed accurately with a relative gap that does not exceed 2.8%. However, At the moment of a sudden change in the real signal, an overflow is observed for the reconstructed signal. It is also noted that when a fault occurs for the rotor speed sensor, a perturbation appears in the signal reconstructed for the generator speed sensor fault, and vice versa, due to the fact that the two quantities are coupled by (5) and (6).

Case 3: The rotor speed sensor fault is also simulated. It starts at 1,400 s and ends at 1,600 s as shown in Figure 4 (fault case 3), and the fault amplitude is 0.2 rad/s, which is 20% of the maximum measured rotor speed value. A part from the overshoot at the time of state change, and the disturbance in the interval (400, 600 s) due to the fault in the rotor speed sensor which occurs in this interval, the rotor speed sensor fault is reconstructed with good accuracy, the relative gap is: 2.5%.

Case 4: The fault profile of the pitch position sensor is shown in Figure 4 (fault case 4). Starting at 1,100 s and ending at 1,200 s, with a maximum amplitude of 0.8°. The real signal and their reconstructed values are perfectly confused.

Case 5: In this case, the sensor faults are considered simultaneously. Figure 5 illustrates this situation: the generator speed sensor and rotor speed sensor faults are considered between 400 and 600 s, the generator torque sensor fault starts at 510 s and ends at 680 s, and the pitch position sensor fault is considered between 520 and 650 s. The simulation results show that the generator torque sensor and pitch position sensor faults are reconstructed accurately. The overshoot is still observed for the generator speed sensor and rotor speed sensor faults; however, the relative gaps for these two faults are respectively evaluated at 0.08% and 0.07%, which shows that the reconstruction accuracy is higher compared to the case of the faults considered separately. This allows us to conclude that the effect of the modification brought to the observer, already evoked in paragraph 3.2, is more significant in the case of simultaneous faults.

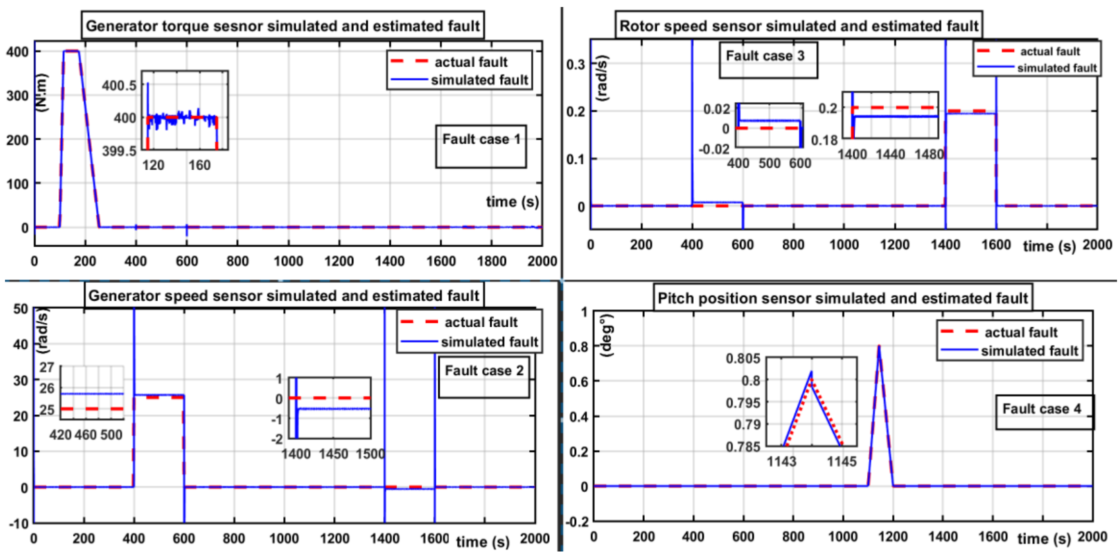

Figure 4. Actual and estimated faults, case of separately faults (fault cases 1-4)

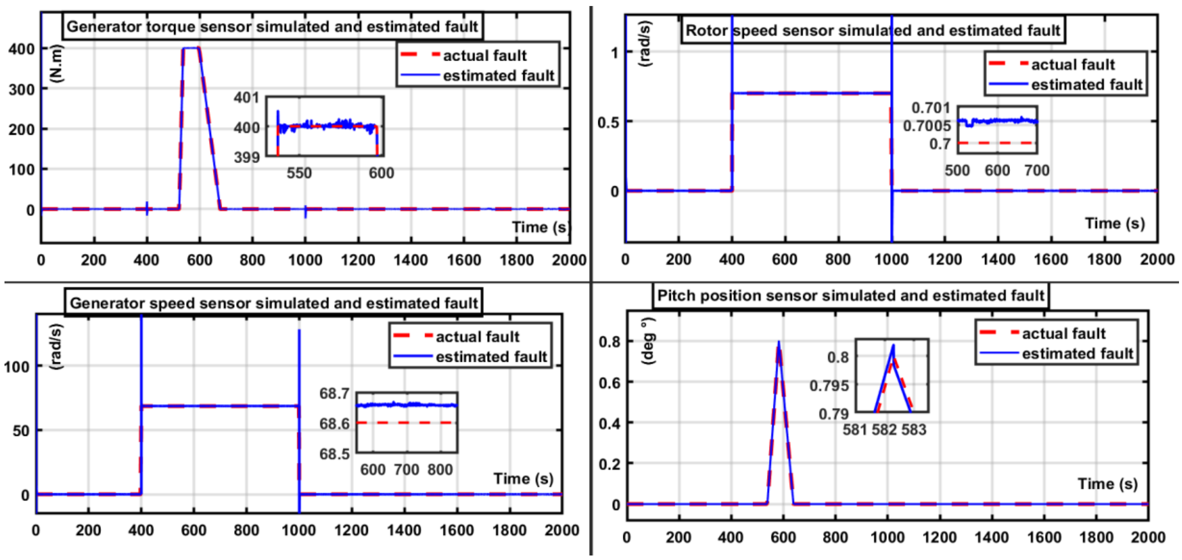

Figure 5. Actual and estimated faults, case of simultaneous faults (fault case 5)

5. CONCLUSION

The wind turbine faults affecting the generator torque sensor, generator speed sensor, rotor speed sensor, and pitch angle sensor result in non-optimal operation of the wind turbine system. In this paper, a sliding mode observer with a modified switching term to fit the different magnitudes of the sensor faults is implemented in order to reconstruct in real time the aforementioned faults. To validate the proposed modification, five sensor fault scenarios are proposed. These scenarios illustrate two situations: in the first one, the faults are considered individually, and in the second one, the faults are considered simultaneously. Throughout the simulation, the switching term is taken to be of the same value even though the sensor faults have quite different magnitudes. The results of the simulation show that the faults are detected, isolated, and reconstructed with precision in the situation of the faults considered individually, except for the overshoot observed for the generator speed and rotor speed sensor faults, which disappears in a very short time. In the case of the simultaneous faults (case 5), the reconstruction is more precise and done without changing the parameters of the SMO, which justifies the modification of the switching term proposed for this SMO.

REFERENCES

[1] J. Brożyna, W. Strielkowski, A. Fomina, and N. Nikitina, “Renewable energy and EU 2020 target for energy efficiency in the Czech Republic and Slovakia,” *Energies*, vol. 13, no. 4, Feb. 2020, doi: 10.3390/en13040965.

[2] S. Yu, Y. Zheng, and L. Li, “A comprehensive evaluation of the development and utilization of China’s regional renewable energy,” *Energy Policy*, vol. 127, pp. 73–86, Apr. 2019, doi: 10.1016/j.enpol.2018.11.056.

[3] V. Akbari, M. Naghashzadegan, R. Kouhikamali, F. Afsharpanah, and W. Yaïci, “Multi-objective optimization and optimal airfoil blade selection for a small horizontal-axis wind turbine (HAWT) for application in regions with various wind potential,” *Machines*, vol. 10, no. 8, Aug. 2022, doi: 10.3390/machines10080687.

[4] A. Al Noman, Z. Tasneem, M. F. Sahed, S. M. Muyeen, S. K. Das, and F. Alam, “Towards next generation Savonius wind turbine: Artificial intelligence in blade design trends and framework,” *Renewable and Sustainable Energy Reviews*, vol. 168, Oct. 2022, doi: 10.1016/j.rser.2022.112531.

[5] B. Wu, Y. Lang, N. Zargari, and S. Kouro, *Power conversion and control of wind energy systems*. Hoboken, NJ, USA: John Wiley & Sons, Inc., 2011.

[6] P. F. Odgaard, J. Stoustrup, and M. Kinnaert, “Fault tolerant control of wind turbinesa benchmark model,” *IFAC Proceedings Volumes*, vol. 42, no. 8, pp. 155–160, 2009, doi: 10.3182/20090630-4-ES-2003.00026.

[7] P. F. Odgaard, J. Stoustrup, and M. Kinnaert, “Fault-tolerant control of wind turbines: a benchmark model,” *IEEE Transactions on Control Systems Technology*, vol. 21, no. 4, pp. 1168–1182, Jul. 2013, doi: 10.1109/TCST.2013.2259235.

[8] W. Chen, S. X. Ding, A. Haghani, A. Naik, A. Q. Khan, and S. Yin, “Observer-based FDI schemes for wind turbine benchmark,” *IFAC Proceedings Volumes*, vol. 44, no. 1, pp. 7073–7078, Jan. 2011, doi: 10.3182/20110828-6-IT-1002.03469.

[9] Y. Fu, Z. Gao, Y. Liu, A. Zhang, and X. Yin, “Actuator and sensor fault classification for wind turbine systems based on fast fourier transform and uncorrelated multi-linear principal component analysis techniques,” *Processes*, vol. 8, no. 9, Sep. 2020, doi: 10.3390/pr8091066.

[10] X. Zhang, Q. Zhang, S. Zhao, R. Ferrari, M. M. Polycarpou, and T. Parisini, “Fault detection and isolation of the wind turbine benchmark: an estimation-based approach,” *IFAC Proceedings Volumes*, vol. 44, no. 1, pp. 8295–8300, Jan. 2011, doi: 10.3182/20110828-6-IT-1002.02808.

[11] C. Li, J. Teng, T. Yang, and Y. Feng, “Adaptive observer based fault detection and isolation for wind turbines,” in *2020 Chinese Automation Congress (CAC)*, Nov. 2020, pp. 481–486, doi: 10.1109/CAC51589.2020.9327557.

[12] C. P. Tan and C. Edwards, "Sliding mode observers for robust detection and reconstruction of actuator and sensor faults," *International Journal of Robust and Nonlinear Control*, vol. 13, no. 5, pp. 443–463, Apr. 2003, doi: 10.1002/rnc.723.

[13] A. A. Ozdemir, P. Seiler, and G. J. Balas, "Wind turbine fault detection using counter-based residual thresholding," *IFAC Proceedings Volumes*, vol. 44, no. 1, pp. 8289–8294, Jan. 2011, doi: 10.3182/20110828-6-IT-1002.01758.

[14] H. Alwi, C. Edwards, and C. P. Tan, "Sliding mode observers for fault detection," in *Advances in Industrial Control*, Springer London, 2011, pp. 53–98.

[15] X. Sun, "Unknown input observer approaches to robust fault diagnosis," University of Hull, 2013.

[16] N. Laouti, S. Othman, M. Alamir, and N. Sheibat-Othman, "Combination of model-based observer and support vector machines for fault detection of wind turbines," *International Journal of Automation and Computing*, vol. 11, no. 3, pp. 274–287, Jun. 2014, doi: 10.1007/s11633-014-0790-9.

[17] N. Sheibat-Othman, S. Othman, M. Benlahrache, and P. F. Odgaard, "Fault detection and isolation in wind turbines using support vector machines and observers," in *2013 American Control Conference*, Jun. 2013, pp. 4459–4464, doi: 10.1109/ACC.2013.6580527.

[18] F. Shi and R. Patton, "An active fault tolerant control approach to an offshore wind turbine model," *Renewable Energy*, vol. 75, pp. 788–798, Mar. 2015, doi: 10.1016/j.renene.2014.10.061.

[19] R. Rahimilarki, Z. Gao, N. Jin, and A. Zhang, "Convolutional neural network fault classification based on time-series analysis for benchmark wind turbine machine," *Renewable Energy*, vol. 185, pp. 916–931, Feb. 2022, doi: 10.1016/j.renene.2021.12.056.

[20] M. Xu, J. Li, S. Wang, N. Yang, and H. Hao, "Damage detection of wind turbine blades by Bayesian multivariate cointegration," *Ocean Engineering*, vol. 258, Aug. 2022, doi: 10.1016/j.oceaneng.2022.111603.

[21] C. Edwards and S. K. Spurgeon, "On the development of discontinuous observers," *International Journal of Control*, vol. 59, no. 5, pp. 1211–1229, May 1994, doi: 10.1080/00207179408923128.

[22] J. C. L. Chan, T. H. Lee, and C. P. Tan, "A sliding mode observer for robust fault reconstruction in a class of nonlinear non-infinitely observable descriptor systems," *Nonlinear Dynamics*, vol. 101, no. 2, pp. 1023–1036, Jul. 2020, doi: 10.1007/s11071-020-05843-9.

[23] M. Mousavi, M. Rahnavard, and S. Haddad, "Observer based fault reconstruction schemes using terminal sliding modes," *International Journal of Control*, vol. 93, no. 4, pp. 881–888, Apr. 2020, doi: 10.1080/00207179.2018.1487082.

[24] J. Lan, R. J. Patton, and X. Zhu, "Fault-tolerant wind turbine pitch control using adaptive sliding mode estimation," *Renewable Energy*, vol. 116, pp. 219–231, Feb. 2018, doi: 10.1016/j.renene.2016.12.005.

[25] S. Georg and H. Schulte, "Diagnosis of actuator parameter faults in wind turbines using a Takagi-Sugeno sliding mode observer," in *Advances in Intelligent Systems and Computing*, Springer Berlin Heidelberg, 2014, pp. 29–40.

[26] M. Rahnavard, M. R. Hairi Yazdi, and M. Ayati, "On the development of a sliding mode observer-based fault diagnosis scheme for a wind turbine benchmark model," *Energy Equipment and Systems*, vol. 5, no. 1, pp. 13–26, 2017.

[27] M. Rahnavard, M. Ayati, and M. R. H. Yazdi, "Robust actuator and sensor fault reconstruction of wind turbine using modified sliding mode observer," *Transactions of the Institute of Measurement and Control*, vol. 41, no. 6, pp. 1504–1518, Apr. 2019, doi: 10.1177/0142331218754620.

[28] C. Sloth, T. Esbensen, and J. Stoustrup, "Robust and fault-tolerant linear parameter-varying control of wind turbines," *Mechatronics*, vol. 21, no. 4, pp. 645–659, Jun. 2011, doi: 10.1016/j.mechatronics.2011.02.001.

[29] H. Alwi, C. Edwards, and C. P. Tan, *Fault detection and fault-tolerant control using sliding modes*. Springer, 2011.

BIOGRAPHIES OF AUTHORS

Mohammed Taouil received his master's degree in electronics and communications systems at the Oujda Faculty of Science in 2008. He is currently a Ph.D. student in the Laboratory of Electronic and Embedded Systems (LES), Team of Embedded Systems, Renewable Energy, and Artificial Intelligence, National School of Applied Sciences, Mohammed Premier University, Oujda, Morocco. His research interests include wind energy and photovoltaic energy. He can be contacted at email: t123med@hotmail.fr.

Abdelghani El Ougli received his Ph.D. degree in Automation, Signals, and Systems from the Faculty of Sciences at Dhar el-Mehraz, University of Sidi Mohamed Ben Abdellah, in 2009 for his thesis titled "Integration of Fuzzy Techniques in the Synthesis of Adaptive Controllers". He is currently a professor at Sidi Mohamed Ben Abdellah University, a researcher, and a member of the team of the Computer Science, Signal, Automation, and Cognitivism Laboratory (LISAC), Faculty of Science, Sidi Mohamed Ben Abdellah University, Fez, Morocco. He can be contacted at email: a.elougli@yahoo.fr.

Belkassem Tidhaf is currently a professor and the head of the Department of Information Technology and Communication Networks at the National School of Applied Sciences at Mohammed first university in Oujda, Morocco. He is a researcher and a member of the Team of Embedded Systems, Renewable Energy, and Artificial Intelligence at the National School of Applied Sciences, Mohammed first university, Oujda, Morocco. He can be contacted at email: tidhaf@yahoo.com.

Hafida Zrouri received her Ph.D. degree for her thesis titled "Study of the electronic transport properties of transition metals and liquid alloys". She is currently a professor, a researcher, and a member of the Laboratory of Electroncs and Systems (LES), Team of Embedded Systems, Renewable Energy, and Artificial Intelligence, at the Superior School of Technology in Oujda, Morocco. She can be contacted at email: zrouri@yahoo.fr.